MIXED CONVECTION FROM ELECTRONIC EQUIPMENT COMPONENT AT DIFFERENT POSITION AN ENCLOUSER BY PRIMITIVE VARABILS METHOD

Dr.Jalal M.Jalil
Mech. Eng. Dept.
Military College of Eng
Assist. Prof.

Dr.Khalid.A.Ismael
Mech. Eng. Dept
Technology University
Prof.

Mr.Sattar J.Habeeb
Mech. Eng. Dept
Technology University
Assist. Teacher

ABSTRACT

A numerical study of mixed conv. . tion cooling of heat dissipating electronic component, located in a rectangular enclosure ,and cooled by an external through flow of air is carried out .A conjugate problem is solved by primitive variables method, describing the flow and thermal fields in air .The interaction between the components is of interest here, depending on their relative placement in the enclosure, and different configuration are considered. for $Re=100$ laminar, steady flow is predicted for up to $Gr/Re^2=25$ according to heat source location in the enclosure. The mixed convection regime, where the buoyancy effects are comparable to the forced flow, occurs at values of Gr/Re^2 between 0.01 and 25 .The results are of values in search for suitable placement of electronic components in an enclosed region for an effective heat removal. In general , it appears that the location of the source on the left vertical wall is the most favorable in terms of cooling. Laminar results are predicted up for up to $Gr=2.5*10^5$ for all configurations studied .

الخلاصة

تم دراسة تشتيت الحرارة الناتجة من أداء الأجهزة الإلكترونية الموضوعة داخل تجويف مستطيل الشكل ، من اجل تبريدها بواسطة هواء خارجي يسلط عليها، مما يؤدي إلى الاستفادة من انتقال الحرارة بالحمل المختلط الناتج من ذلك. حيث تمت الدراسة باستخدام الحل العددي التقريبي لمعادلات الكتلة والزخم والطاقة عن طريق وصف الحركة الديناميكية والحرارية للمائع. أن عملية التداخل الناتجة من وجود اكثر من مصدر حراري داخل الحيز المدروس هي المسألة المهمة هنا ، اعتمادا على موقع المصادر الحرارية نسبتا بعضها إلى البعض الأخر داخل التجويف المستطيل الشكل . كما تم أخذ تغير موقع المصادر الحرارية داخل الحيز بنظر الاعتبار ، بالنسبة $Re=100$ ، جريان طباقي، مستقر، إلى رقم ريشاردسون Gr/Re^2 بحدود 25 طبقا إلى موقع المصدر الحراري داخل الحيز. في منطقة الحمل المختلط فأن تأثير قوى الطفو قورنت نسبة إلى حالة الحمل القسري والتي تتكون لرقم ريشاردسون بين 25 – 0.01. النتائج كانت لقيم البحث عن افضل موقع للمصدر الحراري داخل الحيز عن طريق تأثير إزالة الحرارة .بصورة عامة أتضح أن وضع المصدر الحراري على الجدار العلوي الأيسر

للحيز المدروس يعطي أفضل أداء لعملية التبريد وإزالة الحرارة.كما كانت قيم رقم كراشوف بحدود $Gr = 2.5 * 10^5$ لكل الحالات المدروسة .

KEY WORDS
cooling of electronic component ,mixed convection , CFD ,simulation , enclosure .

INTRODUCTION

An area which has seen a considerable amount of research activity in the recent years is that of heat removal for electronic equipment with the continued effort to decrease the size of electronic equipment , the energy dissipated per unit area has increased substantially in most engineering applications . Air cooling is still the most attractive method for computer system and other electronic equipment ,due to its simplicity and low cost . Thermal engineers in the electronics industry are always trying to achieve the best possible performance out of air cooling . In this effort , the need to understand the variety of flow phenomena and convective heat transfer mechanisms that are present in air - cooled electronic systems is obvious.

A number of studies on the convective heat transfer in enclosure , such as solar collection systems , room ventilation and electronic circuit have been extensively reported regarding the cooling process. Recently, considerable attention has turned to mixed convection problems owing to many practical applications including cooling of electronic equipment and devices {G.P. Paterson and A. Ortega 1990 },{K.J. Kennedy and A. Zabib 1983}. In an enclosure , the interaction between the external forced stream and buoyancy driven flow induced by the increasing high heat flux from electronic module leads to the possibility of complex flow. Therefor its important to understand the heat transfer characteristics of mixed convection in the enclosure.

Mixed convection flow and heat transfer has been studied for inclined channels with discrete heat sources {C.Y. Choi and A. Ortega 1993 } , { C. Yucel , H. Hasnaoui, L. Robillard , and E. Bilgen 1993}. It is found by Choi that the best performance in heat transfer is obtained when the channel is in a vertical location . The Yucel is pointed out that the normalized Nusselt number is a decreasing function of the Reynolds number and an increasing function of the inclined angle .{ E. Papanicolaou and Y. Jaluria 1990 and 1993} studied mixed convection from an isolated heat source in a rectangular enclosure . They indicated that flow patterns generally consist of high- or low- velocity recirculating Celia due to buoyancy forces generated by the heat source .

In addition, the effect of the thermal conductivity of the cavity walls on the heat transfer phenomena was investigated by Jaluria . A later investigation { E. Papanicolaou and Y. Jaluria 1995} further presented turbulent flow in a cavity by **k-ε** model . Turbulent results were obtained for $Re = 1000$ and 2000 , in the rang of $Gr = 5*10^7$ to $5*10^8$. A detailed study of mixed convection in a partially divided rectangular enclosure was presented by { T.H. Hsu ,P.T. Hsu , and S.P. How 1997 }. It was observed that the heat transfer coefficient decrease rather rapidly as the height of the partition is more than about half of the total height of the enclosure . In the present work , therefore , where a enclosure configuration is considered , with protruding heat sources at various locations , the following conditions are considered :-

1- convection heat transfer in the enclosure only .
2- protruding heat sources (blocks) in the enclosure, mounted on surfaces that are either parallel or perpendicular to each other.
3- Interaction between a buoyancy – induced flow and a forced flow whose direction is perpendicular to the gravity vector.

The geometry of the cavity and the relevant parameters considered here are shown in **Fig(1),** for the study of the conjugate problem. The walls are assumed to be small thickness therefor the conduction through it can be neglected .The total dimensions Htot ,Wtot include the corresponding dimensions of the air – filled cavity plus the thickness of the walls.

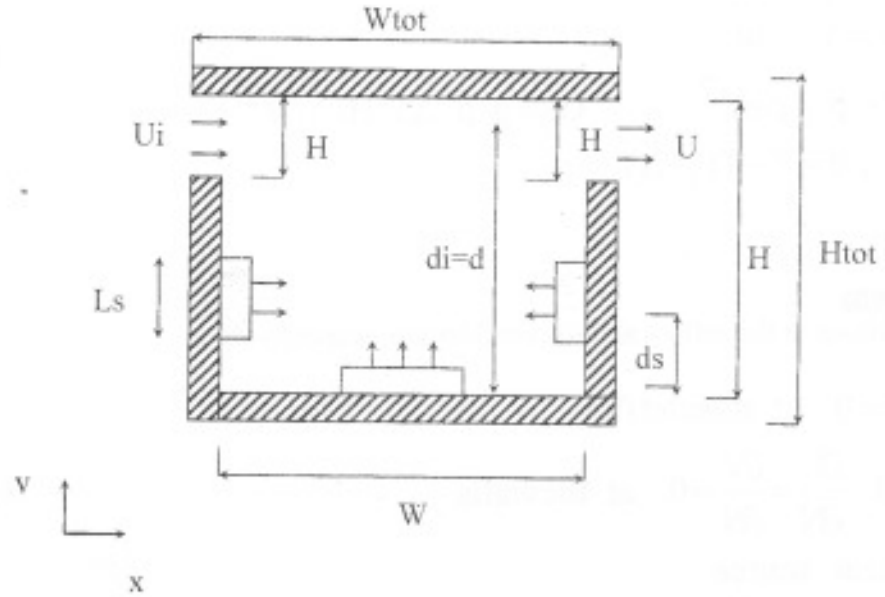

Fig.(1).Physical model of the gavity.

The configuration shown in **Fig.(1)** is a generic case , including three location of the sources , corresponding to the left , right and the bottom side walls . This case will be referred to as LRB for brevity from now on . However, most different locations and the corresponding configurations will be, respectively , named as LR (for sources on the left and right walls) , LB (left and bottom walls) , and RB (right and bottom walls) configuration s .The heat sources will be referred to as L , R, and B depending on their respective location .
The two dimensional problems is studied here , where each heat source actually represented a row of electronic components , sufficiently long in the third dimension .

MATHEMATICAL FORMULATION

Model Equations

The equation describing the problem for the configuration of **Fig.(1)** are the Navier-Stokes equations for the fluid , with buoyancy effect taken into account , as well as the energy equation , which describes the temperature variation through the fluid (air) , the flow assumed to be steady , laminar , and incompressible.
The nondimensional equations can be written as :-

$$\frac{\partial U}{\partial X} + \frac{\partial V}{\partial Y} = 0 \qquad (1)$$

$$U\frac{\partial U}{\partial X} + V\frac{\partial U}{\partial Y} = -\frac{\partial P}{\partial X} + \frac{1}{Re}\nabla^2 U \qquad (2)$$

$$U\frac{\partial V}{\partial X} + V\frac{\partial V}{\partial Y} = -\frac{\partial P}{\partial Y} + \frac{1}{Re}\nabla^2 V + \frac{Gr}{Re^2}\theta \qquad (3)$$

$$U\frac{\partial \theta}{\partial X} + V\frac{\partial \theta}{\partial Y} = \frac{1}{Re \bullet Pr}\nabla^2 \theta \qquad (4)$$

Where the above equation are non dimensionalized by using the dimensionless parameters defined as :-

$$X = x / Hi \quad , \quad Y = y / Hi$$
$$U = u / ui \quad , \quad V = v / ui$$
$$Pr = \nu / \alpha \quad , \quad P = p / \rho ui^2 \quad ; \quad Gr = g.\beta.\Delta T.Hi^3 / \nu^2 \qquad (5)$$
$$Re = ui.Hi / \nu \quad , \theta = T - Ti / \Delta T$$
$$\Delta T = Th - Ti$$

Boundary Conditions

The boundary conditions at the inflow and the outflow are, respectively :-

$$Ui=1,\ Vi=0\ ,\ \theta i=0 \quad \text{at the inlet flow.}$$
$$U=0,\ V=0 \quad \text{and} \quad \frac{\partial U}{\partial N}=\frac{\partial V}{\partial N}=0 \quad \text{at the walls.} \qquad (6)$$
$$\theta i=1 \quad \text{at the heat source}$$
$$\frac{\partial U}{\partial N}=\frac{\partial V}{\partial N}=\frac{\partial \theta}{\partial N}=0 \quad \text{at the exit flow (smoth exit)}$$

The sensitivity of the solution to the outflow boundary conditions was tested by Papanicolaou and Jaluria{5}.The mean Nussult number define as :-

$$\overline{Nu} = \int_0^1 \frac{1}{\theta(y)}\, dy \qquad (7)$$

NUMERICAL METHOD

Governing Eqs.(1- 4) were solved numerically by the primitive variables method (finite volume method) to obtain steady state laminar flow solution , with hybrid scheme approximation for the convective terms {J.P. Simoneau , C. Inard , and F. Allard 1988}. The second upwind and central differencing scheme were also used for comparison and no significicent differences were found .

To determine the appropriate grid size with which grid independent solutions can be Obtained , the calculation were done on increasingly finer grid size distributions. A 21*21 uniform grid with a denser clustering near the walls was considered to give – independent result . To corroborate this the 21*21 grid results were compared with the solution on an 42*48 uniform grid . The two results compare very well with each other with a maximum local difference of 4.5% in the two solutions. The general transport equation for laminar flow in cartesian coordinates may be presented by :

$$\frac{\partial(\rho\Phi)}{\partial t}+\frac{\partial(\rho\Phi U_i)}{\partial X_i}=\frac{\partial}{\partial X_i}\left(\Gamma_\Phi\frac{\partial\Phi}{\partial X_i}\right)+S_\Phi$$

where

$i = 1,2,3$

$\frac{\partial(\rho\Phi U_i)}{\partial X_i}$ = convection term

$\frac{\partial}{\partial X_i}\left(\Gamma_\Phi\frac{\partial\Phi}{\partial X_i}\right)$ = diffusion term (8)

S_Φ = source term

where Φ is the dependent variable . **Table (1)** gives the expressions for the source terms S_Φ for each variable that is likely to be needed in solving cooling problems .

Table (1) Source Terms in the Transport Equations.

Equation	Φ	Γ_Φ	S_Φ
Conntinuity	1	μ	0
Momentum	U1 = U	μ	$-P_X+1/3(\mu\nabla.U)+\rho g_x$
Momentum	U2 = U	μ	$-Py+1/3(\mu\nabla.U)+\rho gy$
Momentum	U3 = U	μ	$-Pz+1/3(\mu\nabla.U)+\rho gz$
Temperature	T	Γ	Q/Cp

μ : dynamic viscosity , Γ : diffusion coefficient (diffusivity)

If we use the Boussinesque approximation, we get :-

$\rho g_x = \rho g_z = 0$

$$\rho g_y = -g\left(1-\frac{\Delta T}{T}\right) \quad \text{where} \quad \Delta T = T - Tr \tag{9}$$

Tr = Reference Temperature

Solution of Governing Equations

Most of the reviewed material solve the models using the finite volume based methods. The most frequent scheme used in solving the air flow was the SIMPLE scheme and some of its variations (SIMPLEC etc...). Most investigators used the hybrid method (central / upwind Differencing), for solving the transport equation, In the following sections the equations are first discretized using finite volume methods, then a suitable difference scheme is applied. The solution process is finally concluded with the method of applying the boundary conditions.

Discretization Methods

To solve the governing equations numerically they must be discretized and formulated in such a way to preserve there nature. Two main methods of discretization are the finite element and finite difference methods. The use o f the finite element method was thought to be much better since it offers greater flexibility specially for difficult geometries. Finite difference schemes are widely used , and are the more common . Complex geometry's can be modeled when generalized

coordinates are used. Finite difference scheme may be derived either by using the Taylor expansion polynomial approximation or by the use of the finite volume scheme.

Finite Volume Method (Control Volume)

The basic idea of the control volume (CV) formulation is to divide the domain into a number of non-overlapping CV's such that there is one CV surrounding each grid point. The differential equation is integrated over each CV , {H.K . Versteeg and W. Malalasekera 1995 } .The most attractive f-ature of the CV formulation is that the resulting solution would imply that the integral conservation of quantities such as mass, momentum and energy is exactly satisfied over each and any group of CV's and of course over the whole computational domain.

This characteristic exists for *any* number of grid points , not just in a limiting sense when the number of grid points becomes large. Then , even the coarse-grid solution exhibits *exact* integral balances.

Two Dimensional Discretization

The general transport equation may be written as,

$$\frac{\partial(\rho\Phi)}{\partial t}+\frac{\partial}{\partial X_i}\left(J_i\right)=S_\Phi \qquad (10)$$

where $J_i=\rho U_i\Phi-\Gamma_\Phi\frac{\partial\Phi}{\partial X_i}$

Ji represents all the flux due to both diffusion and convection . The source term may be expressed as a linear expression :-

$$S_\Phi=b\Phi_p+c \qquad (11)$$

Note the pressure term is excluded from the source term (in the momentum equation) in the solution procedure , and the linearization is done for all other terms only .

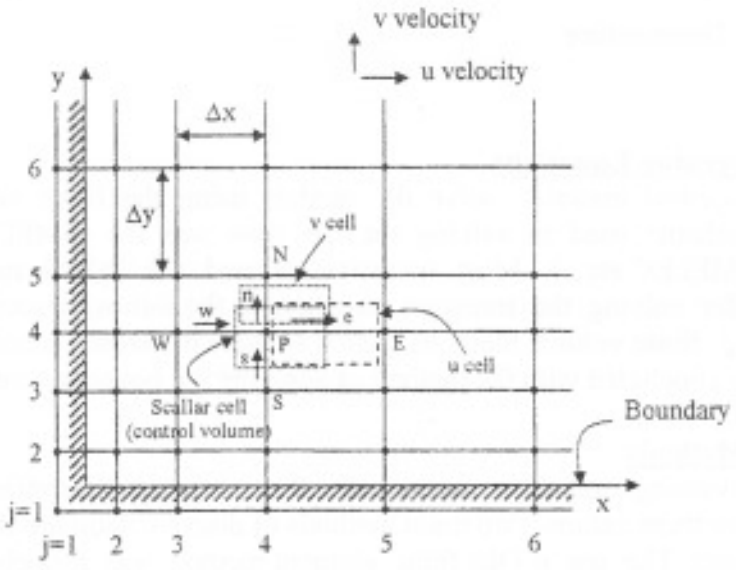

Fig.(2). Grid and control volume for 2D field (H.K. Versteeg).

Integrating using the CV we get ,

$$\left(\rho_p\Phi_p - \rho_p^o\Phi_p^o\right)\Delta A/\Delta t + J_e - J_w + J_n - J_s = \left(b\Phi_p + c\right)\Delta A \qquad (12)$$

where n (north) and s(south) are the neighbouring points of p in the y-direction , $\Delta A=\Delta X^* \Delta Y$ is the area of the CV, and the J's are the integrated total fluxes. Integrating the continuity gives,

$$\left(\rho_p - \rho_p^o\right)\Delta\rho/\Delta t + F_e - F_w + F_n - F_s = 0 \qquad (13)$$

where the F's are the mass flow rates through the control surfaces. The ..... two-dimensional discretization equation can be obtained from eq.(12) and eq.(13), and is given by,

$$\left(\sum_i a_i + a_p^o - b\right)\Phi_p = \sum_i a_i\Phi_i + c \qquad (14)$$

where

$$\sum_i a_i = a_p = a_e + a_w + a_n + a_s$$

$$\sum_i a_i\Phi_i = a_e\Phi_e + a_w\Phi_w + a_n\Phi_n + a_s\Phi_s \qquad (15)$$

$$a_p^o = \rho_p^o\,\Delta A/\Delta t$$

$$b = S_p\Delta A$$

$$c = S_u\Delta A + a_p^o\Phi_p^o$$

Applying any scheme to solve this will give the values of ai , for instance if the Hybrid scheme is used ,

$$a_e = \langle 0, D_e - 0.5|F_e|\rangle + \langle 0, -F_e\rangle$$

$$a_w = \langle 0, D_w - 0.5|F_w|\rangle + \langle 0, F_w\rangle \qquad (16)$$

$$a_n = \langle 0, D_n - 0.5|F_n|\rangle + \langle 0, -F_n\rangle$$

$$a_s = \langle 0, D_s - 0.5|F_s|\rangle + \langle 0, F_s\rangle$$

The convection and diffusion fluxes are given by,

$$F_e = (\rho U)_e\Delta y \quad \& \quad D_e = \Gamma_e\Delta y/\delta x_e$$

$$F_w = (\rho U)_w\Delta y \quad \& \quad D_w = \Gamma_w\Delta y/\delta x_w \qquad (17)$$

$$F_n = (\rho U)_n\Delta x \quad \& \quad D_n = \Gamma_n\Delta y/\delta y_n$$

$$F_s = (\rho U)_s\Delta x \quad \& \quad D_s = \Gamma_s\Delta y/\delta y_s$$

All the coefficients in eqs. (15) and (16) are used for solving for (Temperature , kinetic and dissipation , ..), the velocity components are calculated on a staggered grid and there values differ.

RESULTS AND DISCUSSION

Definition of Physical and Geometric Parameters

The results to be presented here will focus on the effect of certain parameters , while keeping the others fixed. More specifically , the parameters listed below in dimensionless

form , chosen to represent a cavity that would most likely appear in an electronic system , although not exclusively so , are kept fixed at the following values see **Fig(1)).**
Aspect ratio of the air – filled cavity $A = H^*/W^* = 1$, $Hi^* = Ho^* = Ls^* = 1$, $di^*/H^* = do^*/H^* = 0.8571$ The distance of the center of the sources from the bottom of the cavity is taken such that $ds^*/H^* = 0.357$, while on the bottom wall the corresponding distance is $ds^*/W^* = 0.5$, measured from the left vertical wall. The parameters to be varied here the Grashof number , the number of the sources , and the relative locations of the sources. All the alternative cases will be compared to each other. The Reynolds number is being kept fixed in this work at $Re = 100$, a value representative of the laminar regime , characterizing on incoming flow of a relatively low velocity. For instance, an air flow of about 0.1 m /s ,entering through an opening 2 cm height at $20\,c^\circ$ would yield a Reynolds number of the above – mentioned order of magnitude .Higher values of Re have been considered before {Jaluria 1990}, and the basic flow in the cavity were not affected significantly as long as $Re \leq 1000$ The Grashof number is varied in the range $Gr = 10^3 - 2.5 * 10^5$ and this effect will be presented .

In what follows , as a variation in the Richardson number Gr/Re^2 over the corresponding range . Gr/Re^2 Is a more suitable parameter in mixed convection problems and since the Reynolds number is kept fixed , varying the value of Gr/Re^2 will be equivalent to varying the heat input from the sources. Generally , the Grashof number encountered in electronic cooling are of the order of 10^5 or higher, but in this case ,in order to get a more complete picture of the effect of Gr/Re^2 on the heat transfer, the rang of Gr has been extended to lower values.

Flow and thermal field for steady mixed convection

Fig.(3,4,5) shows the velocity vector in the enclosure at different values of Richardson number $Gr/Re^2 = 5$ and 25 of fixed value of $Re = 100$ and different location of heat source (LR , LB , RB) .

All these cases leads to steady laminar solution. The flow field shows unicellular pattern at $Gr/Re^2 = 5$, but at this value a secondary flow develops due to the buoyancy effects from source R , at the base of the right side wall . At $Gr/Re^2 = 25$, the secondary cell becomes bigger and occupies more of the space originally belonging to primary cell . The temperature field (Isotherm contours , **Fig(6,7,8)**) in the fluid adjacent to source L exhibits the characteristics of a natural convection boundary layer a plumelike pattern of isotherms at all values of Gr/Re^2 chosen while for source R such a pattern makes its appearance for $Gr/Re^2 = 5$, source R is shown to be subject to an opposing recirculating flow.

For the same values of Re and Gr/Re^2 as before , the corresponding results for the LB configuration as shown in **Fig(4)** the buoyancy induced flows due to both the sources are now in the same direction ,aiding the recirculating flow .Therefore a unicellular flow pattern is observed at all values of Gr/Re^2 , with the recirculation gradually increasing with an increase in Gr/Re^2 . Thermal boundary layers are clearly observed over both sources, the BR configuration gives rise to a variety of flow patterns, as seen **in Fig(5) .**

At $Gr/Re^2 = 5$, the external flow dominates over the buoyancy effects and the flow field resembles the one generated in a driven cavity. At a higher buoyancy level , $Gr/Re^2 = 25$, the buoyancy effects from source B again add to the recirculation of the original cell , while the secondary cell is now due to buoyancy effect from the source R only and is restricted to a region

form , chosen to represent a cavity that would most likely appear in an electronic system , although not exclusively so , are kept fixed at the following values see **Fig(1)).**
Aspect ratio of the air – filled cavity $A = H^*/W^* = 1$, $Hi^* = Ho^* = Ls^* = 1$, $di^*/H^* = do^*/H^* = 0.8571$ The distance of the center of the sources from the bottom of the cavity is taken such that $ds^*/H^* = 0.357$, while on the bottom wall the corresponding distance is $ds^*/W^* = 0.5$, measured from the left vertical wall. The parameters to be varied here the Grashof number , the number of the sources , and the relative locations of the sources. All the alternative cases will be compared to each other. The Reynolds number is being kept fixed in this work at $Re = 100$, a value representative of the laminar regime , characterizing on incoming flow of a relatively low velocity. For instance, an air flow of about 0.1 m /s ,entering through an opening 2 cm height at $20\,c^\circ$ would yield a Reynolds number of the above – mentioned order of magnitude .Higher values of Re have been considered before {Jahria 1990}, and the basic flow in the cavity were not affected significantly as long as $Re \leq 1000$ The Grashof number is varied in the range $Gr = 10^3 - 2.5 * 10^5$ and this effect will be presented .

In what follows , as a variation in the Richardson number Gr/Re^2 over the corresponding range . Gr/Re^2 Is a more suitable parameter in mixed convection problems and since the Reynolds number is kept fixed , varying the value of Gr/Re^2 will be equivalent to varying the heat input from the sources. Generally , the Grashof number encountered in electronic cooling are of the order of 10^5 or higher, but in this case ,in order to get a more complete picture of the effect of Gr/Re^2 on the heat transfer, the rang of Gr has been extended to lower values.

Flow and thermal field for steady mixed convection

Fig.(3,4,5) shows the velocity vector in the enclosure at different values of Richardson number $Gr/Re^2 = 5$ and 25 of fixed value of $Re = 100$ and different location of heat source (LR , LB , RB) .

All these cases leads to steady laminar solution. The flow field shows unicellular pattern at $Gr/Re^2 = 5$, but at this value a secondary flow develops due to the buoyancy effects from source R , at the base of the right side wall . At $Gr/Re^2 = 25$, the secondary cell becomes bigger and occupies more of the space originally belonging to primary cell . The temperature field (Isotherm contours , **Fig(6,7,8)**) in the fluid adjacent to source L exhibits the characteristics of a natural convection boundary layer a plumelike pattern of isotherms at all values of Gr/Re^2 chosen while for source R such a pattern makes its appearance for $Gr/Re^2 = 5$, source R is shown to be subject to an opposing recirculating flow.

For the same values of Re and Gr/Re^2 as before , the corresponding results for the LB configuration as shown in **Fig(4)** the buoyancy induced flows due to both the sources are now in the same direction ,aiding the recirculating flow .Therefore a unicellular flow pattern is observed at all values of Gr/Re^2 , with the recirculation gradually increasing with an increase in Gr/Re^2 . Thermal boundary layers are clearly observed over both sources, the BR configuration gives rise to a variety of flow patterns, as seen **in Fig(5) .**

At $Gr/Re^2 = 5$, the external flow dominates over the buoyancy effects and the flow field resembles the one generated in a driven cavity. At a higher buoyancy level , $Gr/Re^2 = 25$, the buoyancy effects from source B again add to the recirculation of the original cell , while the secondary cell is now due to buoyancy effect from the source R only and is restricted to a region

adjacent to the right vertical wall , this change in the flow patterns and the direction of the buoyancy-induced flow from source B can be seen in the isotherm plots(**Fig(8)**).

Average Nusselt number $\overline{Nu}$:-

Fig(9) shows the relative magnitude of the average Nusselt number $\overline{Nu}$ at the sources for mixed convection over the corresponding value for forced convection $\overline{Nuf}$, at different values of Gr/Re^2 , can be plotted , as shown in **Fig(9)** . Generally, the ratio $\overline{Nu}/\overline{Nuf}$ increase with Gr/Re^2 except in BR configuration at low Gr/Re^2 .In that case , the opposing effects of the external flow are stronger and $\overline{Nu}/\overline{Nuf}$ decreases , first with Gr/Re^2 , before buoyancy dominates and an increasing trend is observed .

This behavior was also found in the opposing forced – flow results of {11}, where the Nusselt number curves crossed the forced convection asymptote as Gr/Re^2 decrease before approaching the asymptote value. The results can be decribed by a correlation of the following form :-

$$\frac{\overline{Nu}}{\overline{Nuf}} \alpha \left(\frac{Gr}{Re^2}\right)^c \qquad (8)$$

Where c depends on the configuration and the source location and has the computed values shown in **Table (2) .**

Table (2) Magnitude of C Parameter.

CONFIGURATION	SOURCE LOCATION	C
LR	L	0.0518
LR	R	0.0248
RB	R	0.2463
RB	B	0.2391
LB	L	0.6906
LB	B	0.1859

All these have correlation coefficients close to 0.99 . It can be observed in table above , that in the LB configuration the variation of the Grashof number has a much larger effect on the heat transfer compared to the other two configuration .

CONCLUSION

A numerical procedure was developed to simulate the laminar mixed convection cooling of electronic components located in an enclosure . Results are presented for the flow field and temperature distribution in the fluid (air). The numerical method presented is very robust and capable of treating different numbers , locations of heat sources.

In general , it appears that the location of the source on the left vertical wall is the most favorable in terms of cooling . Laminar results are predicted up for up to $Gr = 2.5 * 10^5$ for all configurations studied .

The two-dimensional model studied here applies to two or three long rows of electronic modules mounted on either one of two vertical printed circuit boards or on a horizontal board and extending in the direction normal to the plane under consideration . The results from

the various cases studied are extremely helpful in understanding the flow patterns that develop in an air – cooled electronic enclosure and the thermal interactions between the components, this allows for an evaluation of the various alternative placements of the components and selection of the one that leads to the best thermal performance. Quantitative heat transfer result were also obtained and compared to previously existing data for configuration of relevance to the present ones.

REFERENCES

C.Y. Choi and A. Ortega , (1993), Mixed Convection in an Inclined Channel with a Discrete Heat Source; Int. J. Heat Mass Transfer , vol. (36) , no.(2), pp.(3119-3134) .

E. Papanicolaou and Y. Jaluria, (1990), Mixed Convection from an Isolated Heat Source in Rectangular Enclosure ; Numerical Heat Transfer , Part (A), vol. (18) , pp.(427-461) .

E. Papanicolaou and Y. Jaluria, (1993), Mixed Convection from a Localized Heat Source in a Cavity with Conducting Walls; A Numerical study , Numerical Heat Transfer , Part (A), vol. (17) , pp(463-484)

E. Papanicolaou and Y. Jaluria, (1995), Computation of Turbulent flow in Mixd Convection in a Cavity with a Localized Heat Source ; ASME J. Heat Transfer , vol. (17) , pp(649-658) .

G.P. Paterson and A. Ortega, (1990) , Thermal Control of Electronic Equipment and Devices Advance Heat Transfer , vol. (20) , pp.(181- 314).

H.K. Versteeg and W.Malalasekera, (1995), An Introduction to Computational Fluid Dynamics , The Finite Volume Method,

J.P. Simoneau , C. Inard , and F. Allard , (1988), Numerical Approach to Interaction Between an Injection and Laminar Natural Convection in a thermal Driven Cavity; ASME. HTD. Vol. (99) , pp.(45-51).

K.J. Kennedy and A. Zebib, (1983), Combined Free and Forces Convection between Horizontal Parallel Plates ; Int. J. Heat Mass Transfer , vol. (26), no.(3), pp.(471-474) .

L. Robillard C. Yucel, H. Hasnaoui , and E. Bilgen, (1993), Mixed Convection Heat Transfer in Open Ended Inclined Channels with Discrete Isothermal Heating; Numerical Heat Transfer , Part (A), vol. (24) , pp.(109-126) .

Patankar S.V. , (1980), Numerical Heat Transfer and fluid flow , Hemisphere, Washington, DC .

T.H. Hsu , P.T. Hsu ,and S.P. How, (1997), Mixed Convection in a Partially Divided Rectangular enclosure ; Numerical Heat Transfer , Part (A), vol.(31) , pp(655-683) .

NOMENCLATURE

A	Area
a	Coefficient values
D	Diffusion factor at control surface
d	Vertical distance from the bottom of the enclosure

e,w,n,s	Values at east,west,north,south
F	Flow rate at control volume
Gr	Grashof number
Gr/Re^2	Richardson number
g	Acceleration of gravity (body force)
H	Height of air-filled cavity
Hi , Ho	Height of the inflow and outflow channels
J	Flux due to both diffusion and convection
Ls	Length of the heat sources
$\overline{Nu}$	Average Nusselt number in mixed convection
$\overline{Nuf}$	Average Nusselt number in forced convection
P	Dimensionless local pressure
Pr	Prandtl number
Re	Reynolds number
S_Φ	Heat source
T	Physical temperature
ΔT	Temperature scale (Th-Ti)
U , V	Dimensionless horizontal and vertical velocity
Ui	Mean value of the horizontal velocity component at the inflow
W	Width of air-filled cavity
X ,Y	Dimensionless horizontal and vertical coordinate in general form equal N

GREEK NOMENCLATURE

Φ	Dependent variable
α	Thermal diffusivity
β	Coefficient of thermal expansion
θ	Dimensionless temperature
ν	Kinematic viscosity

SUBSCRIPTS

i	Inflow
o	Outflow
h	Hot location
C	Cold location
*	Dimensionless quantities

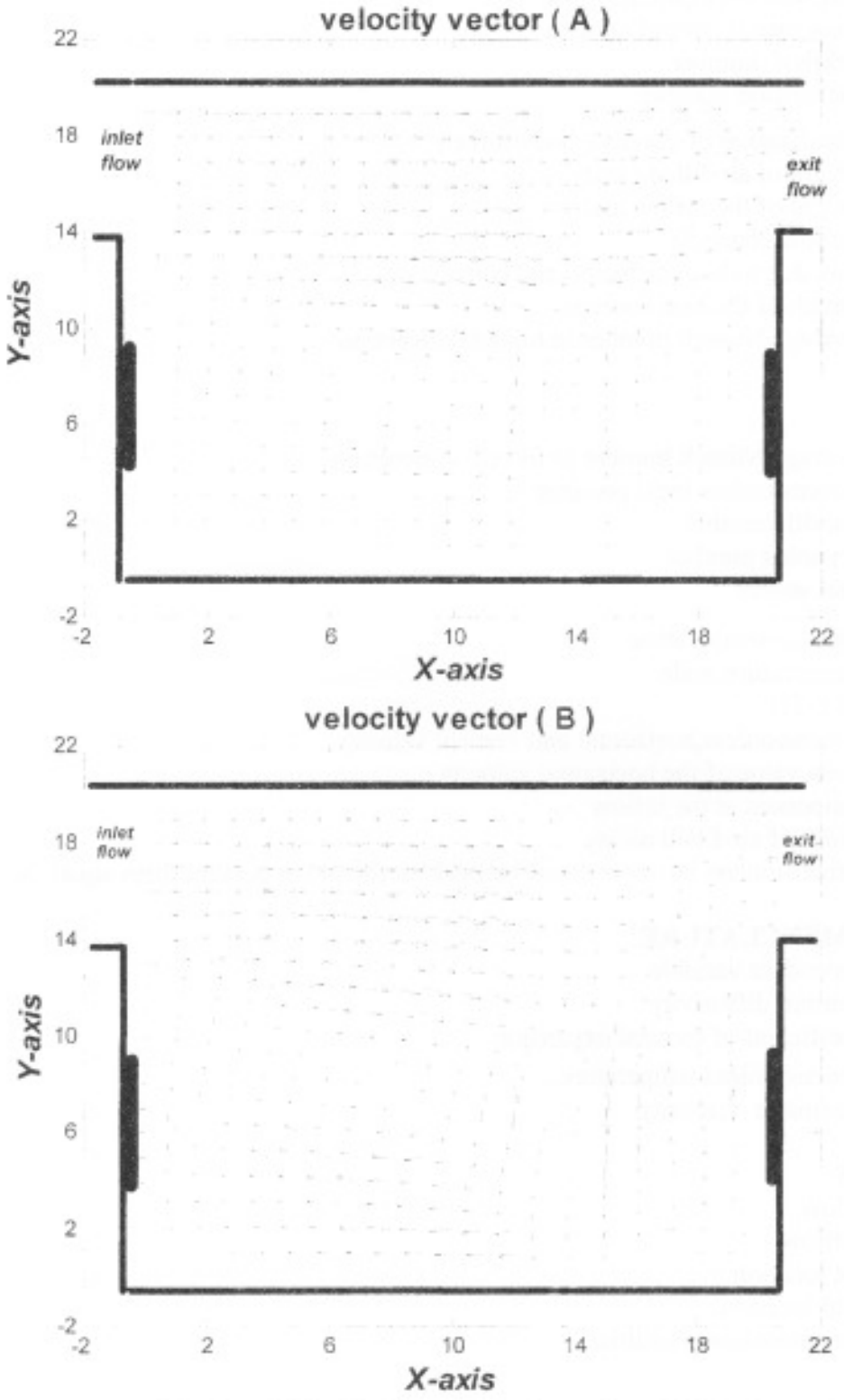

Fig.(3) Velocity Vector of the Flow Field in the Enclosure when the Location of the Heat Sources in the Left and Right Walls:

(A) Gr/Re^2 =5 and Re=100 (B) Gr/Re^2 =25 and Re=100

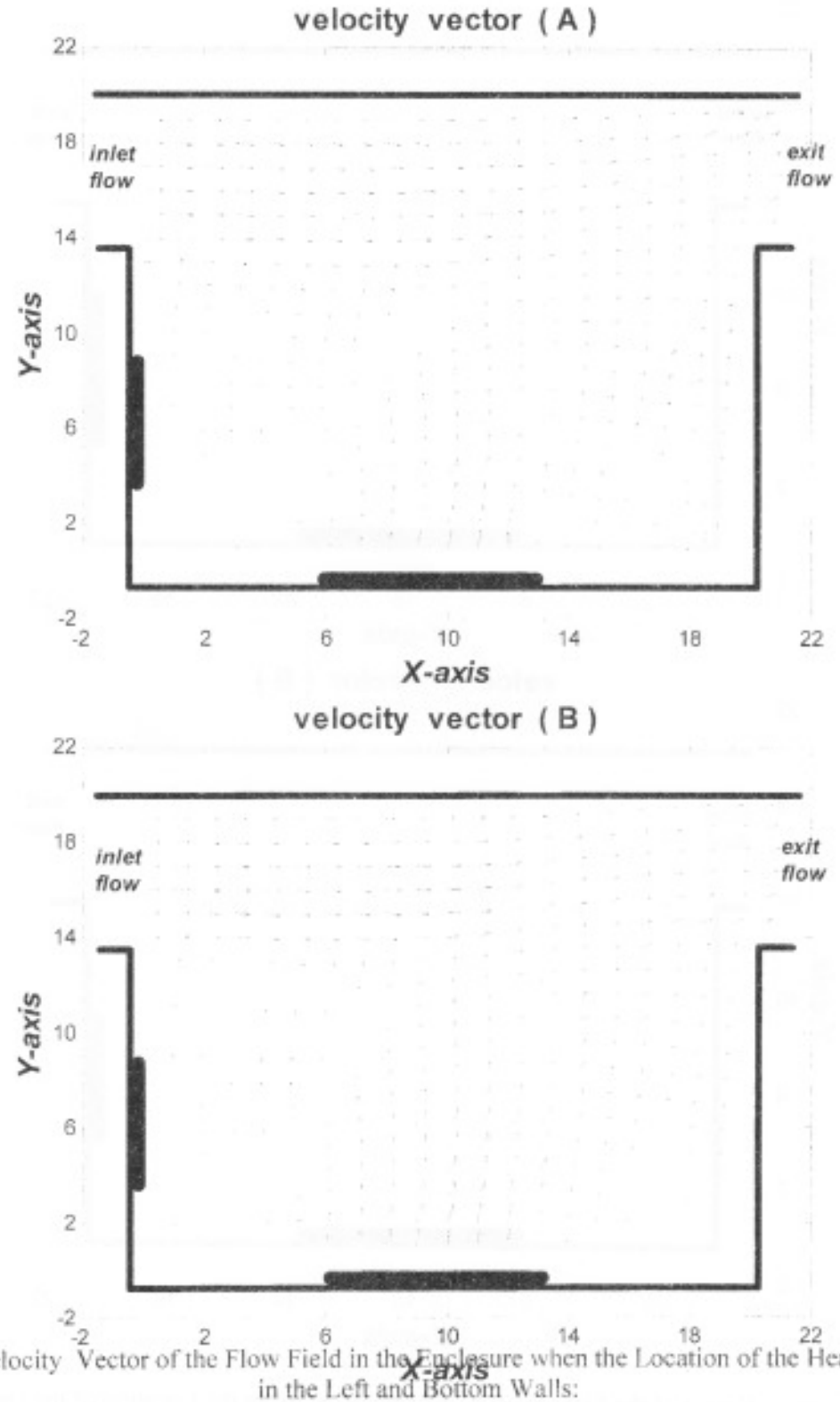

Fig.(4) Velocity Vector of the Flow Field in the Enclosure when the Location of the Heat Sources in the Left and Bottom Walls:

(A) Gr/Re^2 =5 and Re=100 (B) Gr/Re^2 =25 and Re=100

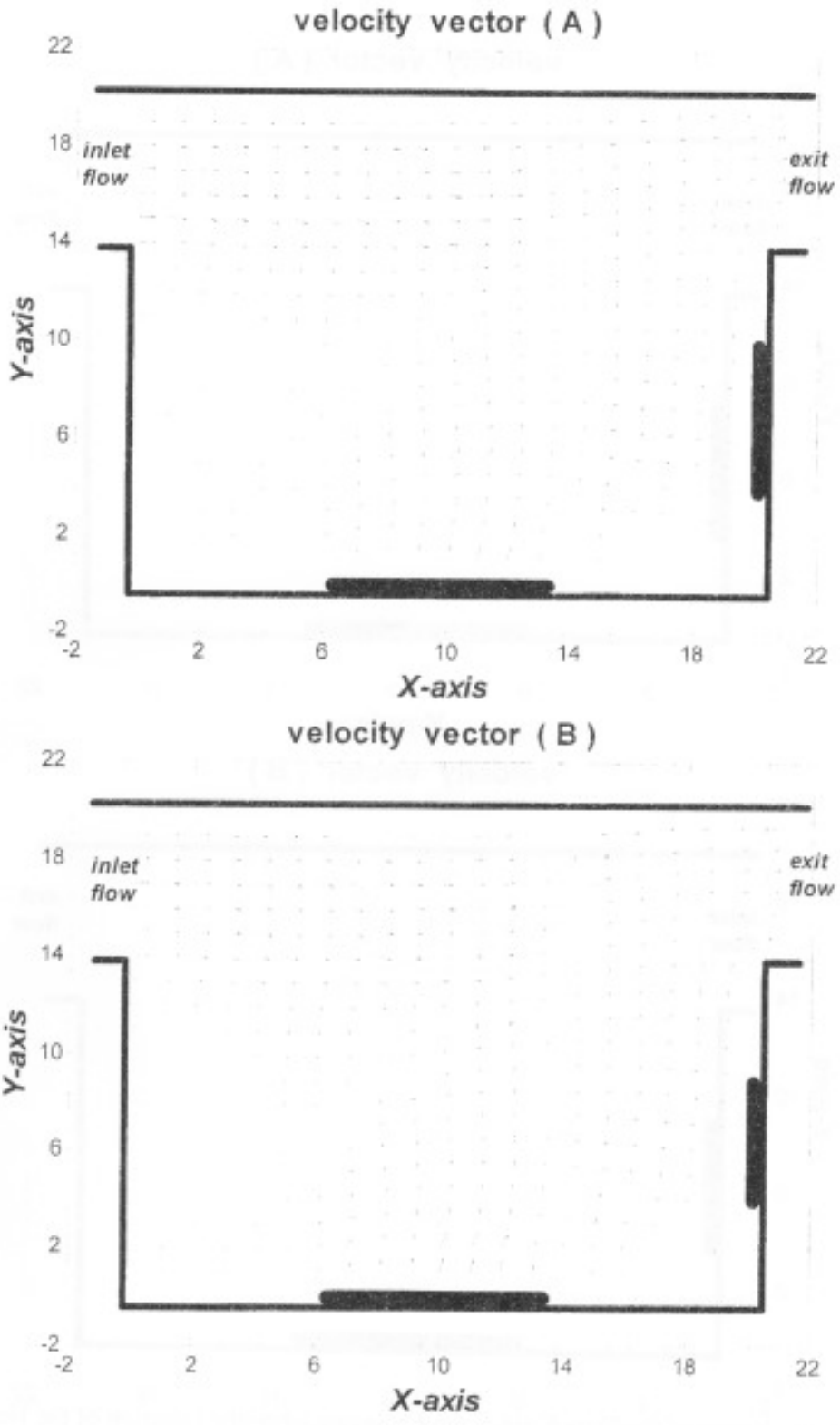

Fig.(5) Velocity Vector of the Flow Field in the Enclosure when the Location of the Heat Sources in the Right and Bottom Walls:

(A) Gr/Re^2 =5 and Re=100 (B) Gr/Re^2 =25 and Re=100

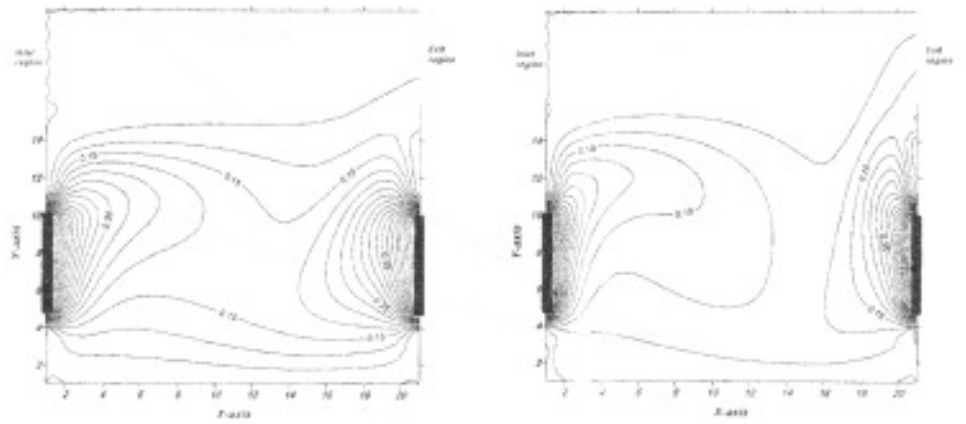

(A) (B)

Fig.(6) Isotherms Contours in LR Configuration, for Re=100 and
(A) Gr/Re^2 =5 (B) Gr/Re^2 =25.

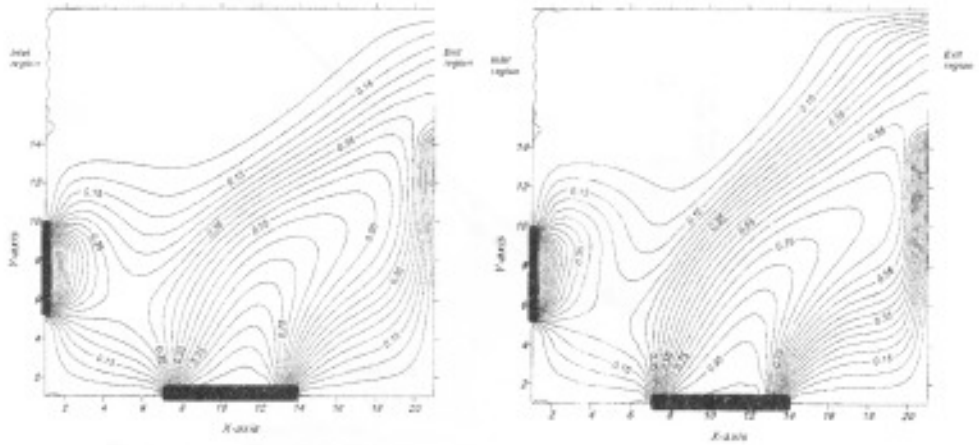

(A) (B)

Fig.(7) Isotherms Contours in LB Configuration, for Re=100 and
(A) Gr/Re^2 =5 (B) Gr/Re^2 =25.

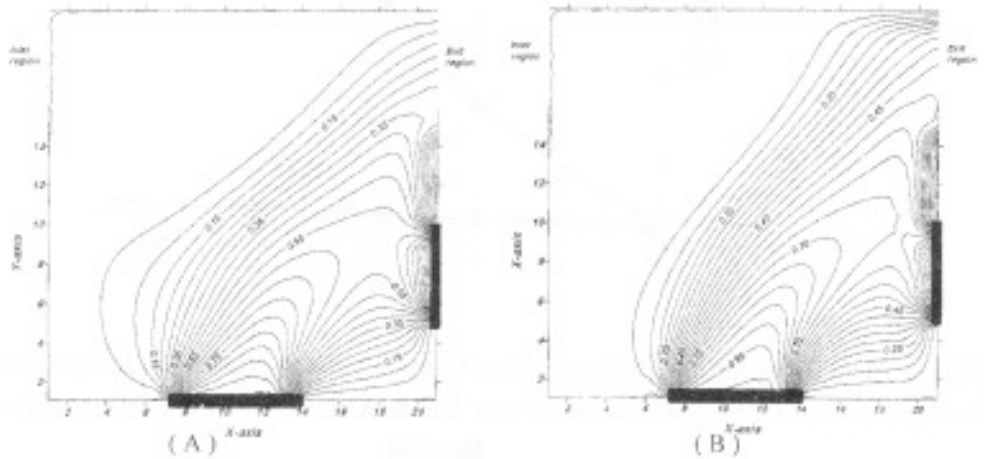

(A) (B)

Fig.(8) Isotherms contours in RB configuration, for Re=100 and
(A) Gr/Re^2 =5 (B) Gr/Re^2 =25.

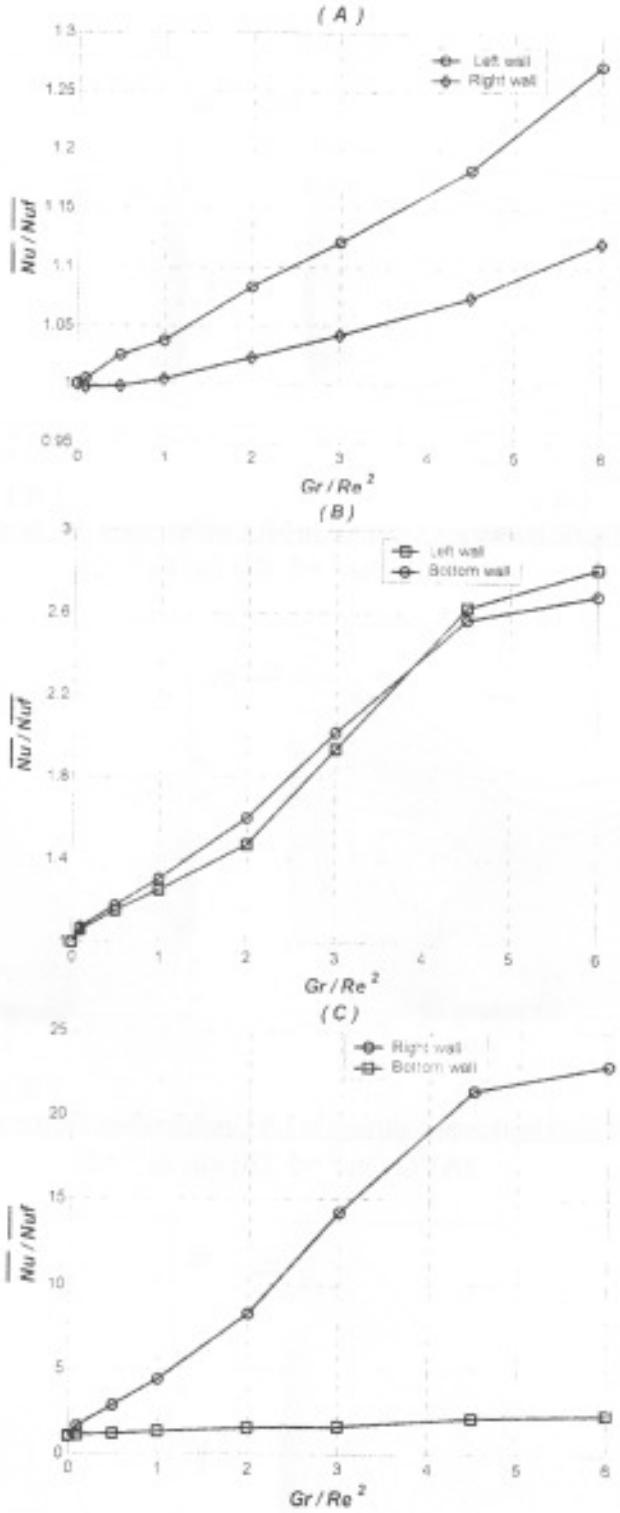

Fig.(9) The Variation of the Ratio of the Average Nusselt Number at the Source in Mixed Convection $\overline{Nu}$. to the Forced Convection Value $\overline{Nuf}$. at Various Values of Gr/Re^2 and **Re=100**

(A) LR configuration. (B) LB configuration. (C) RB configuration.